3 Biotech (2023) 13:318
https://doi.org/10.1007/s13205-023-03726-5

ORIGINAL ARTICLE

Formulation of lemongrass oil (*Cymbopogon citratus*)-loaded solid lipid nanoparticles: an in vitro assessment study

Abuzer Ali[1] · Amena Ali[2] · Musarrat Husain Warsi[3] · Wasim Ahmad[4] · Mohd Amir[5] · Sayed Aliul Hasan Abdi[6]

Received: 18 April 2022 / Accepted: 1 August 2023 / Published online: 26 August 2023

Abstract

Cymbopogon citratus (DC) stapf. (Gramineae) is a herb known worldwide as lemongrass. The oil obtained, i.e., lemongrass oil has emerged as one among the most relevant natural oils in the pharmaceutical industry owing to its extensive pharmacological and therapeutic benefits including antioxidant, antimicrobial, antiviral and anticancer properties. However, its usage in novel formulations is constrained because of its instability and volatility. To address these concerns, the present study aims to formulate lemongrass-loaded SLN (LG_{SLN}) using hot water titration technique. In the S_{mix}, Tween 80 was selected as a surfactant component, while ethanol was taken as a co-surfactant. Different ratios of S_{mix} (1:1, 1:2, 1:3, 2:1 and 3:1) were utilized to formulate LG-loaded SLN. The results indicated the fact that the LG_{SLN} formulation (abbreviated as LG_{SLN1}), containing lipid phase 10% w/w (i.e., LG 3.33% and SA 6.67%), Tween 80 (20% w/w), ethanol (20% w/w) and distilled water (50% w/w), revealed suitable nanometric size (142.3 ± 5.96 nm) with a high zeta potential value (− 29.12 ± 1.7 mV) and a high entrapment efficiency (77.02 ± 8.12%). A rapid drug release (71.65 ± 5.33%) was observed for LG_{SLN1} in a time span of 24 h. Additionally, the highest values for steady-state flux (J_{ss}; 0.6133 ± 0.0361 mg/cm^2/h), permeability coefficient (K_p; 0.4573 ± 0.0141 (cm/h) × 10^2) and enhancement ratio (E_r; 13.50) was also conferred by LG_{SLN1}. Based on in vitro study results, the developed SLN appeared as a potential carrier for enhanced topical administration of lemongrass oil. The observed results also indicated the fact that the phyto-cosmeceutical prospective of the nanolipidic carrier for topical administration of lemongrass oil utilizing pharmaceutically acceptable components can be explored further for widespread clinical applicability.

Keywords Lemongrass oil · Particle size analysis · Phase diagram · Solid lipid nanoparticles · Thermodynamic stability

Introduction

In past few years, lemongrass essential oil (*Cymbopogon citratus*; Gramineae) has been the topic of investigation owing to its wide applicability as antioxidant, antimicrobial, antiviral and anticancer agent in the healthcare industries (Mukarram et al. 2021). It is also used as a sedative or as an antimicrobial agent (Al-Harrasi et al. 2022; Souza et al. 2022; Chen and Zhong 2022; Irfan et al. 2022; Faheem et al. 2022) and additionally employed against several species of bacteria, fungi and mycoses (Kumar et al. 2022; Valková et al. 2022). Onawunmi et al. studied the antimicrobial efficacy of lemongrass (LG) oil and further reported that both α-citral (geranial) and β-citral (neral) components have antibacterial activity against gram-negative and gram-positive bacteria (Onawunmi et al. 1984).

LG oil is shown to have antibacterial activity which has led to its usage for the treatment and control of acne

✉ Abuzer Ali
abuali@tu.edu.sa

1 Department of Pharmacognosy, College of Pharmacy, Taif University, P.O. Box 11099, 21944 Taif, Saudi Arabia

2 Department of Pharmaceutical Chemistry, College of Pharmacy, Taif University, P.O. Box 11099, 21944 Taif, Saudi Arabia

3 Department of Pharmaceutics and Industrial Pharmacy, College of Pharmacy, Taif University, P.O. Box 11099, 21944 Taif, Saudi Arabia

4 Department of Pharmacy, Mohammed Al-Mana College for Medical Sciences, 34222 Dammam, Saudi Arabia

5 Department of Natural Products and Alternative Medicine, College of Clinical Pharmacy, Imam Abdul Rahman Bin Faisal University, 34222 Dammam, Saudi Arabia

6 Department of Clinical Pharmacy, Al Baha University, 1988 Al Baha, Saudi Arabia

(Lertsatitthanakorn et al. 2006; Valková et al. 2022). For drugs with systemic side effects, the development of topical drug delivery methods appears to be a suitable and advantageous technique. In such a pursuit, the benefits of topical drug delivery over conventional routes of drug administration are often considered, particularly where localized action is desired. Novel topical drug delivery techniques can help in boosting the delivery of anti-acne agents by enhancing their skin localization while reducing the associated side effects (Zouboulis 2001; Ascenso et al. 2011). In vitro experimental data obtained from conventional dosage forms often yield poor in vivo findings. Insufficient drug concentration upon peroral delivery in standard dosage form could be attributed to poor absorption, metabolism, excretion, poor solubility and excessive variability in plasma concentrations. Delivering the drug using novel drug delivery systems is a prospective approach for overcoming these challenges. There are a few literature reports of some LG-based novel products like nanoemulsion (Salvia-Trujillo 2014), nanoparticle (Masurka 2011) and liposome (Cui et al. 2016). Various investigators have explored the use of solid lipid nanoparticles (SLN) as a suitable option to polymeric and liquid lipid nanoparticles. SLNs are distinguished by their large surface area, increased payload, and the capability to safeguard the enclosed bioactive from the harsh biological atmosphere while improving bioavailability. Because lipidic nanocarriers are very hydrophobic, they are slightly hydrated in aqueous systems, if at all, and so are unable to dissolve or disperse autonomously. As a result, formulating these dispersions necessitates providing energy to the system in order to generate extremely small particles (in the nano-range) with a large specific surface area. Lipophilic drugs with superior lipid compatibility are frequently chosen for incorporation into SLNs for maximum loading of therapeutics (Dolatabadi et al. 2015). High-pressure homogenization technique (Liedtke et al. 2000; Dingler and Gohla 2002; Trotta et al. 2003; Jenning et al. 2002), solvent emulsification or evaporation (Trotta et al. 2003), high-speed stirring ultrasonication and the solvent diffusion method (Yadav et al. 2014; Yuan et al. 2008) are only a few of the techniques used to produce SLNs. For the present study, the hot water titrimetric method was selected to prepare SLN. Hence, the core objective of the current research study was to formulate lipidic nanocarrier-loaded LG oil (LG_{SLN}) by the hot water titrimetric method and to ascertain the physicochemical attributes of the attained formulations.

The present work elaborates upon the potential of a nanolipidic carrier system in cosmeticology for topical delivery of LG oil, using pharmaceutically acceptable ingredients. This study also highlights the ability of SLN as a permeation enhancer.

Material and methods

LG oil was bought from Aroma House, New Delhi, India. Carbitol, Cremophor-EL, Labrasol, Labrafil and plurol oleique were obtained ex-gratia from Gattefosse (Mumbai, India). All other chemicals used were of the AR grade.

Constructing the map of the nanoemulsion-phase

Pseudoternary phase diagrams were developed by utilizing hot water titration techniques to assess the concentration scale of different constituents for the fabrication of nanolipid vehicle (Fig. 1). The LG oil was mixed with the pre-melted solid fat (stearic acid) on water bath. S_{mix} (containing Tween 80 and Ethanol) was added into the lipidic mixture (Table 1). The external aqueous medium for titration was distilled water (maintained at a higher temperature in the same hot water bath). Different ratios of components of S_{mix} (1:0, 1:1, 1:2, 1:3, 2:1, 3:1 and 4:1) were selected for the trials. For a thorough overview of phase diagrams to track nanolipidic formulations, these S_{mix} ratios were determined by raising the co-surfactant concentration for surfactant and vice versa. Oil phase (LG)/stearic acid (SA): 1:2 and appropriate S_{mix} were blended in different ratio stretching 1:9 to 9:1 in distinct pre-labeled vials for each phase diagram. A gradual titration using hot water phase was done for each ratio of oil phase and S_{mix}. Water concentrations in the span of 5–95% of overall amount at 5% gaps were achieved by varying the amount of hot water added (Thomas et al. 2017; Zakir et al. 2021). This was done so that the boundaries of the nanoemulsions (NE) and different phases could be properly delineated. The areas of solid NE were clearly obtained on the pseudoternary phase diagram. The different corners of the triangle were having different components of the formulation ingredients like aqueous phase, oil phase and S_{mix}.

Formulation development

SLNs were developed as reported by Muller and Lucks with slight modification (Muller and Lucks 1996; Faiyazuddin et al. 2010a). Pseudoternary diagrams had discrete nanolipidic regions. Different compositions from these regions were selected and the lipidic droplets were crystallized by putting in chilled water (kept at a temperature 6–8 °C) with continuous stirring, which was continued for 45 min to minimize the variation in particle size distribution.

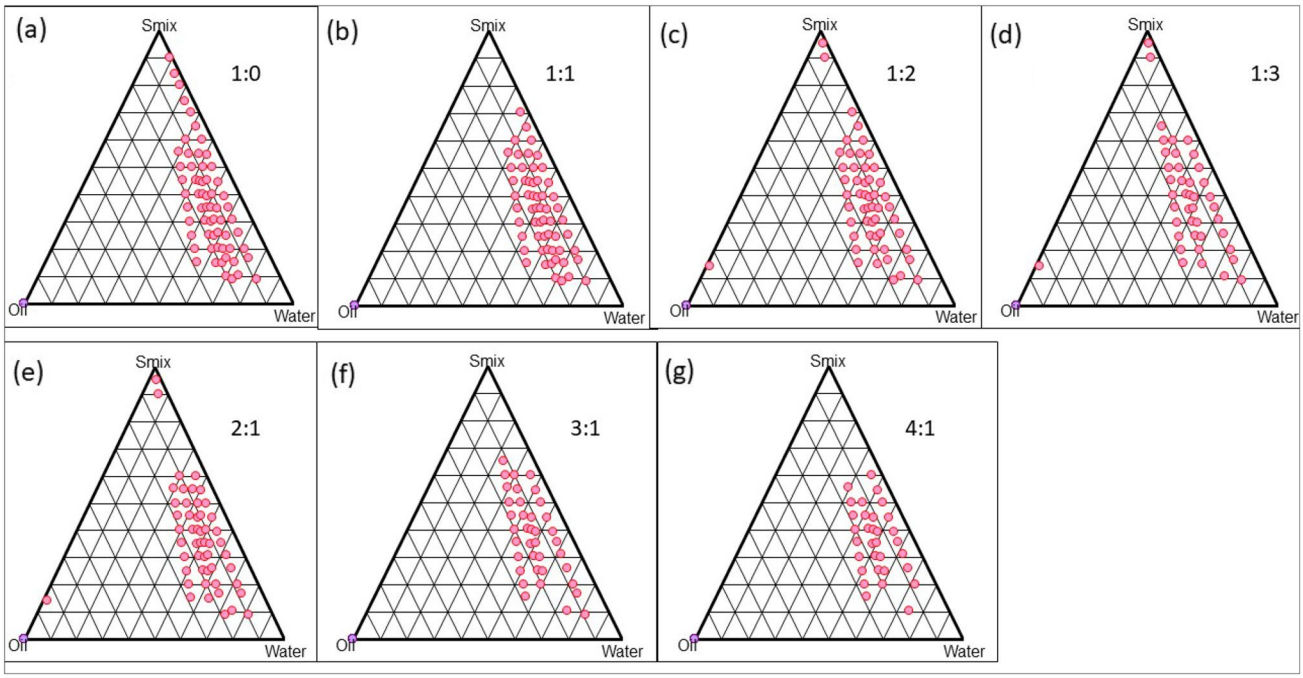

Fig. 1 Phase diagrams indicating o/w nanoemulsion (shaded area) region of oil (LG: SA; 1:2 v/v), surfactant (Tween 80), co-surfactant (ethanol) at different S_{mix} ratios [**a** (S_{mix} 1:0), **b** (S_{mix} 1:1), **c** (S_{mix} 1:2), **d** (S_{mix} 1:3), **e** (S_{mix} 2:1), **f** (S_{mix} 3:1) and **g** (S_{mix} 4:1)]

Table 1 Phase behaviors of lemongrass oil in different surfactants and co-surfactants

Component	Surface area ± SD (cm^2)
Labrafil	57.14 ± 1.65
Labrasol	91.31 ± 2.14
Cremophor-EL	104.23 ± 2.01
Tween 80	266.24 ± 2.52
Tween 20	257.33 ± 1.16
Transcutol P	235.32 ± 1.96
Ethanol	242.54 ± 0.96
Plurol oleique	65.22 ± 1.53

Characterization and optimization of SLN

Thermodynamic stability test Different stress tests of thermodynamic stability studies were used to screen out metastable formulations (Li et al. 2005). Specified formulations were centrifuged for 30 min at a speed of 5000 rpm to check for phase separation, creaming, and cracking. For the heating and cooling cycles, the formulations that demonstrated no phase separation were chosen. Six temperature cycles (4 °C and 45 °C) were selected corresponding to storage conditions for at least 48 h. Freeze thaw was used on the formulations that exhibited stability at the specified stressed temperature. In this investigation, test formulations were thawed thrice at temperatures ranging from − 21 to + 25 °C, maintaining at each temperature for a time period of 48 h (Table 2) (Mirza et al. 2013). Table 3 shows the composition of selected LG-SLN that passed the physical stability tests.

Entrapment efficiency Repeated washings were given to separate out non-entrapped LG from the SLN dispersions (Jaber et al. 2018). The following formula is used to calculate the %entrapment efficiency:

$$\left[(T - S)/T\right] \times 100,$$

where '*T*' is the total amount of entrapped essential oil in the SLN dispersion and '*S*' represents the amount of non-entrapped LG in the dispersion medium. After extraction and dilution with methanol for a time span of 1 h in an ultrasonic bath, EE% was conducted using a UV spectrophotometer at 595 nm. The entrapment efficiency of LG-loaded SLN (LG_{SLN}) is shown in Table 4.

Particle size distribution and zeta potential determination Globule size was calculated by employing a photon correlation spectrometer that analyzes light scattering variations. At a temperature of 25 °C and a 90° angle, the light scattering was analyzed. Droplet size analysis was performed using adequately diluted SLN samples (0.1 mL) diffused in double distilled water (50 mL). The

Table 2 Thermodynamics stability testing of LG-SLN formulations

S_{mix} ratio (S:CoS)	S. no.	Percentage v/v of different components in formulations			Observations based on the thermodynamic stability studies			Inference
		Oil	S_{mix}	Water	H/C	Cent	Freeze	
Oil: Lemon grass + Stearic acid (1:2 v/v), Surfactant: Tween 80, Co-surfactant: Ethanol, External phase: Distilled water								
1:0	1	5	32	63	√	√	√	Passed
	2	5	40	60	√	√	√	Passed
	3	10	38	52	√	x	-	Failed
	4	10	40	50	√	√	√	Passed
	5	15	45	40	√	x	-	Failed
1:1	6	5	30	65	√	√	√	Passed
	7	5	38	57	√	√	√	Passed
	8	10	40	50	√	√	√	Passed
	9	10	43	47	√	√	√	Passed
	10	15	38	52	x	-	-	Failed
1:2	11	5	36	59	√	√	√	Passed
	12	5	41	54	√	√	√	Passed
	13	10	44	46	√	x	-	Failed
	14	10	45	45	√	√	√	Passed
	15	15	47	38	x	√	√	Failed
2:1	16	5	35	60	√	√	√	Passed
	17	5	41	54	√	√	√	Passed
	18	10	42	48	√	x	-	Failed
	19	10	41	49	√	√	√	Passed
	20	15	41	44	x	√	√	Failed
3:1	21	5	38	57	√	√	√	Passed
	22	5	55	40	√	√	√	Passed
	23	10	39	51	√	√	√	Passed
	24	10	50	40	√	√	√	Passed
	25	15	45	40	√	√	x	Failed

H/C heating and cooling (0 °C and 45 °C), *Cent* centrifugation (5000 rpm), *Freeze* freeze–thaw (−21 °C and + 25 °C)

Table 3 Composition of selected LG-SLN that passed the physical stability tests

Formulation code	% Composition of the selected formulation			S_{mix} ratio
	Oil	S_{mix}	Water	
LG_{SLN1}	10	40	50	1:1
LG_{SLN2}	10	43	47	1:1
LG_{SLN3}	10	45	45	1:2
LG_{SLN4}	10	41	49	2:1
LG_{SLN5}	10	39	51	3:1

zeta potential (ZP), polydispersity index (PDI), and average droplet size were measured.

Viscosity The viscosity of the optimized formulations was evaluated using a Brookfield DV III ultra V6.0 RV viscometer with spindle maintained at 25 ± 0.4 °C. Rheocalc V2.6 was used for the analysis (Mirza et al. 2013).

Drug release study

Franz diffusion cell was employed for conducting in vitro drug release study of drug (Bhaskar et al. 2009). Dialysis membrane having a 2.4 nm pore size and the molecular weight cut-off of 12,000–14,000 D was employed for the study. To imitate the pH of the skin, phosphate buffer (pH 5.6) was taken in the receptor compartment. The donor compartment was filled with LG_{SLN} dispersion (1 ml), and the receptor compartment had dissolution media (12 ml). The receptor section was kept at 37 ± 0.5 °C, and the medium was stirred moderately under magnetic stirring. At every predetermined time, 100 µl of the sample was taken out from the receptor compartment via the sampling port, and the same volume was swapped with the fresh medium. The

Table 4 Droplet size distribution, surface charge analysis, rheological study and in vitro drug release of optimized SLN formulations

Formulation code	Droplet size mean ± SD (nm)	Polydispersity index	Zeta potentials ± SD (mV)	Viscosity mean ± SD (cps)	% Entrapment efficiency ± SD	% Drug release (24 h)
LG_{SLN1}	142.3 ± 5.96	0.201	− 29.12 ± 1.7	134.21 ± 3.88	77.02 ± 8.12	71.65 ± 5.33
LG_{SLN2}	168.6 ± 6.01	0.273	− 24.6 ± 2.6	136.26 ± 6.01	67.68 ± 9.86	68.36 ± 7.09
LG_{SLN3}	175.1 ± 8.05	0.367	− 26.2 ± 0.79	138.56 ± 5.22	71.53 ± 9.98	63.97 ± 5.49
LG_{SLN4}	149.4 ± 5.22	0.412	− 28.48 ± 0.92	131.51 ± 8.01	70.24 ± 7.76	52.69 ± 4.79
LG_{SLN5}	205 ± 4.11	0.437	− 34.4 ± 0.76	142.55 ± 6.96	69.79 ± 11.56	48.86 ± 2.42

drug content in the collected samples were analyzed by the developed HPTLC technique at 595 nm against trans-citral of LG (Faiyazuddin et al. 2010a; Ali et al. 2022).

In vitro skin permeation studies

Skin transport experiments were accomplished by the Franz diffusion cell (having surface area 7.16 cm^2 and the capacity of receiver compartment 37 ml) by employing rat abdominal skin. The visceral tissue was removed carefully, and adherent fat was removed by wiping with isopropyl alcohol, which was then rinsed using distilled water and kept at − 21 °C until needed. Then, it was mounted in the receptor compartment of Franz diffusion cell by placing the stratum corneum side toward donor compartment. Ethanolic acetate buffer was taken as receptor medium, and the whole medium was swapped with fresh medium at every 30 min (12 cycles) to stabilize the skin. After placing 1 ml of SLN formulation into donor cell, samples were started to withdraw at definite interval (0.5, 1, 2, 4, 6, 8, 24, 36 and 48 h), then filtered using 0.45-µm syringe membrane filter, and quantified for drug by HPTLC at λ_{max} of 595 nm as reported in previous section. Pure LG oil was taken as control.

Stability study at different storage temperature

For a period of 3 months, short-term stability studies were performed to verify the particle growth potential of the optimized formulations. The SLN dispersion's initial particle size was recorded. The samples were then divided according to three stability conditions, i.e., 4 °C, 25 °C and 50 °C in dark settings. On day 1 and the 90th day, samples were taken out for particle size and zeta potential measurements.

Results and discussion

Screening of components

LG oil was used for the formulation of SLN formulations. In the present study, LG oil has been taken as a drug because there are enough literature reports on its anti-acne, antioxidant, antimicrobial, antiviral and anticancer activities (Holland and Jeremy 2005; Mukarram et al. 2021). The miscibility potential of LG was assessed in solid fats. It was found out that LG was better miscible with stearic acid (SA) (even after cooling; ≤ 8 °C), then comes cetyl alcohol, and glyceryl monostearate. Ratio of liquid and solid lipid was also studied, and a composition (LG: solid fat: 1:2) with SA was taken as the final one. Phasic behavior of LG was also determined in different S_{mix} ratios, as secondary parameters for the screening purpose. The defined phasic surface area of LG was found the highest in Tween 80 (266.24 ± 2.52 cm^2), followed by Tween 20 (257.33 ± 1.16 cm^2), Transcutol (235.32 ± 1.96 cm^2) and ethanol (242.54 ± 0.96 cm^2) (Table 1). Although Transcutol appeared comparable to ethanol, its combination phasic behavior was poor with regard to ethanol. Based on the above findings, Tween 80 (as surfactant) and ethanol (as co-surfactant) were chosen for the S_{mix} composition for the formulation development.

Phase studies for LG oil

Pseudoternary phase diagrams were built by utilizing the hot water titration method at a temperature of 75 ± 0.5 °C. Phase diagram construction is a cumbersome process, especially when there is a target to precisely demarcate a phase limit (Faiyazuddin et al. 2010b). The formation of nanoemulsion is a spontaneous process; hence, the requirement of free energy to drive the process is small (Qadir et al. 2016). Hence, special efforts were made to ensure that no metastable NE system is selected. The pseudoternary phase diagram gives a pictorial view of correlation between phases and composition at each data point. For every S_{mix} ratio, pseudoternary phase diagrams were created independently (Fig. 1a–g), so that oil/water (o/w) nano-provinces could be detected for the optimization of SLN formulations. The S_{mix} ratio of 1:0 (Fig. 1a), 1:1 (Fig. 1b) and 2:1 (Fig. 1e) had a larger nanophase compared to the other S_{mix} ratios. With a high proportion of S_{mix}, an o/w solid NE zone was discovered near the water-rich vertex of the phase diagram. It suggests that Tween 80 is self-sufficient (i.e., co-surfactant

is not required) to develop the nanoemulsion regions but the development of liquid crystalline state indicates to use co-surfactant.

It was observed that S_{mix} 1:0 (Fig. 1a) was unable to efficiently address the surface tension created between oil phase and aqueous phase, so the liquid crystalline area was dominating in the pseudoternary phase diagram. While in the phase diagram of S_{mix} 1:1 (Fig. 1b), the introduction of a co-surfactant appeared to make the film more pliable and the LC zone was visible, compared to Tween 80 alone (Fig. 1a). By utilizing S_{mix} at approximately $69 \pm 0.58\%$ v/v, the maximal proportion of oil that was miscible in the phase diagram (Fig. 1a) was almost $29 \pm 0.37\%$, demonstrating Tween 80's superiority in nanosizing. It was also noted that by raising the concentration in S_{mix} ratio (S_{mix} 1:1–1:3; Fig. 1b–d), there was a slight decline in the nano-phasic region. However, by raising the surfactant concentration in S_{mix} ratios (S_{mix} 2:1–4:1; Fig. 1e–g), a significant increase in nanoemulsion region was noted. The reason behind may be the additional reduction in surface tension between two immiscible liquids and enhanced fluidity/flexibility at the interface, which causes a small increment in the entropy of the system and therefore more assimilation of the oil phase in the hydrophobic zone of the surfactant monomers (Faiyazuddin et al. 2010b). The elaboration of nanophase system was paltry when surfactants attribute in S_{mix} was increased from 3:1 (Fig. 1f). It might be a phase of liquid crystalline produced by Tween-80 and not much supported by the current extent of co-surfactant. The maximum concentration of oil that could be solubilized by these ratios was $31 \pm 0.27\%$ v/v with around $65 \pm 0.18\%$ v/v of S_{mix} (Fig. 1f). The findings are well in sync with the established fact that spontaneity of the nanoemulsion formation depends upon how efficiently the surfactant and co-surfactants lower the oil–water interfacial tension and change the dispersion entropy (Faiyazuddin et al. 2010b; Qadir et al. 2016). In such case, solid NE development is impulsive, and the subsequent dispersions are physically stable (Jenning et al. 2000). When the S_{mix} ratio of 4:1 was studied, no further enhancement in nanoemulsion area was noted, and LC area started to appear into the phase diagrams. The reason behind may be the increased involvement of surfactant. When co-surfactant concentration was increased (1:2, 1:3, etc.), the nano-phasic regions drastically decreased (Fig. 1c, d). For our purposes, those SLNs were chosen with the help of pseudoternary phase diagram in which the quantity of oil phase could be accommodated with the least amount of S_{mix} .

Formulation development

Optimum regions for distinct SLN were exhibited by S_{mix} ratios of 1:1, 1:2, 1:3, 2:1 and 3:1 in pseudoternary phase diagrams. Other S_{mix} combinations were also created, but they were not included in this investigation because of showing very narrow nanophase areas when compared to LC forms. Based on the results of various thermodynamic stability investigations, solid NE preparations with different formulae were chosen from phase diagrams. Almost the whole array of NE incidence in the pseudoternary phase diagrams was studied, and several oil compositions with the lowest concentration of surfactant suggesting the occurrence of NEs were carefully chosen (Table 2). The oil (LG:SA::1:2) and the appropriate quantity of surfactant/co-surfactant were introduced in the stipulated ratio with drop-by-drop hot water until a crystal clear solution was formed, which was then solidified by adding cold water.

Thermodynamic stability test

Solid NEs are developed at a distinct proportion of oil/fat), surfactant ration (S_{mix}) and aqueous phase (Jenning et al. 2000; Mirza et al. 2013). It is a thermodynamically stable system. To get a stable and robust composition, several formulations were exposed to different stressed conditions like centrifugation followed by heating–cooling and freeze–thaw cycle. Physically stable formulations were taken for additional studies. The individual components of all the formulations are given in Table 2.

The basis for the selection of SLN from different compositions was based on the premise having a lesser S_{mix} and higher oil content. The formulation having 5% v/v of oil exhibited superb transparency, but the amount of LG was very less to show pharmacological response. This concept led to raise the drug dose of the formulation. So, every formulation that had a minimum of 10% (v/v) of the oil was selected for the planned study (Table 3).

Optimization and characterization of SLN

Entrapment efficiency A large quantity of LG might be incorporated into the developed SLN, as shown in Table 3. As the drug itself was oil (LG), with the most miscibility in SA, it could be expected to get entrapped up to 100% with the solid lipid. The % entrapment efficiency of the developed formulation was assessed over a period of one month. The mixing of LG with SA led to better entrapment efficiency, i.e., $77.02 \pm 8.12\%$ (LG_{SLN1}); $71.53 \pm 9.98\%$ (LG_{SLN3}); $70.24 \pm 7.76\%$ (LG_{SLN4}); $69.79 \pm 11.56\%$ (LG_{SLN5}); and $67.68 \pm 9.86\%$ (LG_{SLN2}). This is possibly due to the lipophilic nature and higher loading capacity in the optimized formulations. Further, the dual combination of liquid and solid lipids results in decreased order recrystallization (Jenning et al. 2000). The %EE of the LG in nanostructured lipidic carrier was comparable or better than earlier literature reports (Ma et al. 2021; Cui et al. 2016).

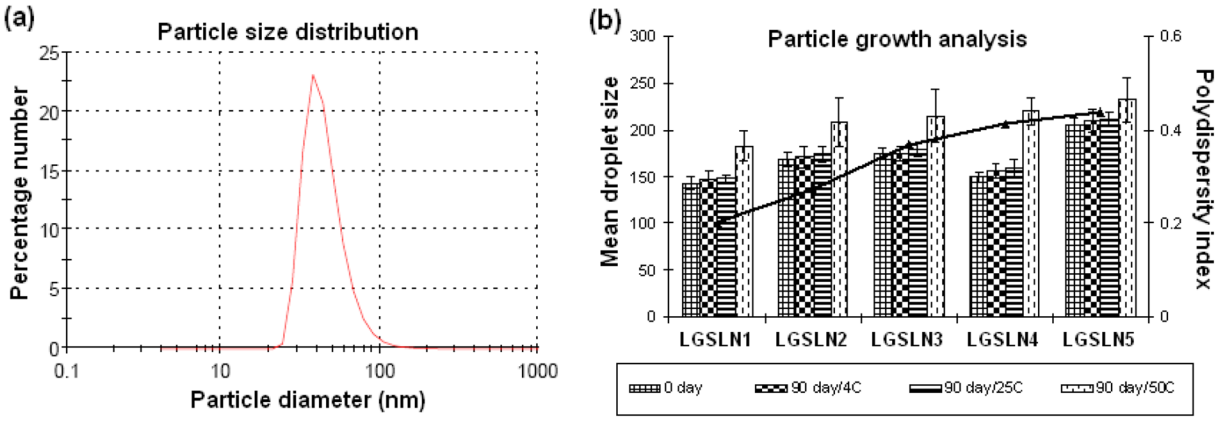

Fig. 2 LG-SLN formulation characterized for **a** particle size distribution and **b** particle growth analysis with polydispersity index at different temperatures

Particle diameter and surface charge analysis The pictorial presentation of distribution of SLN is given statistically in Fig. 2. Table 4 presents the mean droplet size of optimized preparations (LG_{SLN1}–LG_{SLN5}) oscillating from 142 to 205 nm. LG_{SLN5} had the largest droplet size, which can be attributed to the existence of larger concentration of surfactants, which led to enhanced viscosity in the system (Zhao et al. 2017). Due to a lack of co-surfactant concentration, the rigid film was unable to provide additional flexibility for secondary nanosizing. Size analyses of the certain formulations revealed that there is increase in size by increasing the concentration of oil and surfactant. This could be because, even though the variation in droplet size across formulations was statistically insignificant ($p > 0.05$), the current amount of surfactant used was not substantial enough to achieve uniform dispersion at the same S_{mix} ratio (1:1). The PDI was found < 1 for every SLN, which indicates a narrow distribution. LG_{SLN1} showed a minimum PDI (0.201) advocating better uniformity among droplets (Thatipamula et al. 2011). The TEM image of sample is given as supplementary material (S1). The size is not in sync with the particle size analysis. The reason behind may be that in TEM imaging figures are taken from a particular zone of the grid which may or may not capture a particular size range.

It is widely assumed that ZP values of − 30 mV and above characterize a stable system (Jenning et al. 2000). The LG_{SLN1} formulation had the highest ZP (− 29.12 ± 1.7 mV), which remained almost same (with insignificant variation) during the three months period at all temperatures conditions (Table 5), indicating the stable nature of the product. On day first, LG_{SLN1}–LG_{SLN5} formulation showed a ZP value of − 24.6 to − 34.40 mV, and was found to have changed slightly after 3 months (Room temp: 25 °C and 4 °C storage temperature) (Table 5). LG_{SLN1}–LG_{SLN5} when stored at 50 °C showed the change in ZP varying from (− 18.02 to − 21.12 mV) with a drastic change in particle size (Table 5). An experiment by Freitas and Müller, examining the influence of temperature and light on ZP and physical stability in SLNs where poloxamer was taken as a stabilizer, backs up the results as observed at higher temperatures (Freitas and Müller 1999). As a result, it can be deduced that at high temperatures (50 °C), steric stabilizing property conferred

Table 5 In vitro thermal stability studies for selected LG-SLN formulations (Temp: 4°, 25° and 50 °C; day: 0 and 90th day)

Formulation code	Mean droplet size ± SD (nm) and Zeta potential							
	At previous day		After 90 days					
	ZP	PSD	4 °C		25 °C		50 °C	
			PSD	ZP	PSD	ZP	PSD	ZP
LG_{SLN1}	− 29.12 ± 1.7	142.3 ± 5.96	146.6 ± 1.13	− 29.21 ± 0.56	148.5 ± 1.23	− 29.5 ± 1.33	183.19 ± 2.66	− 20.12 ± 2.2
LG_{SLN2}	− 24.6 ± 2.6	168.6 ± 6.01	171.2 ± 0.37	− 30.12 ± 0.17	173.4 ± 1.02	− 31.92 ± 0.31	208.1 ± 0.89	− 19.7 ± 1.13
LG_{SLN3}	− 26.2 ± 0.79	175.1 ± 8.05	176.3 ± 0.11	− 27.96 ± 0.73	181.69 ± 0.39	− 27.91 ± 2.48	214.7 ± 0.89	− 18.02 ± 0.12
LG_{SLN4}	− 28.48 ± 0.92	149.4 ± 5.22	155.7 ± 0.33	− 27.32 ± 1.26	159.4 ± 0.41	− 27.02 ± 1.17	219.8 ± 0.97	− 18.88 ± 0.59
LG_{SLN5}	− 34.40 ± 0.76	205 ± 4.11	207.88 1.97	− 34.01 ± 0.24	212.1 ± 2.11	− 33.19 ± 1.29	231.9 ± 1.88	− 21.12 ± 0.81

ZP zeta potential, *PSD* particle size distribution

by Tween 80 proves to be insufficient which results in particle aggregation.

Viscosity Table 4 presents viscosity data of optimized formulations (LG_{SLN1}–G_{SLN5}) ranging from 131 to 142 cps. The results of viscosity can relate to the distinct roles of the surfactant and co-surfactant taken to stabilize the selected oil ingredient in the formulation. The viscosity of the LG_{SLN1} was almost lowest (134.21 ± 3.88 cps) as compared to other formulations (LG_{SLN2}, LG_{SLN3} and LG_{SLN5}), making it suitable for topical use (i.e., easily washable after use). Notably, the viscosity of the SLN formulations was found quite low. It is one of the hallmarks of this delivery system, i.e., low viscosity (Faiyazuddin et al. 2010b). The low viscosity value is likely attributable to the use of a small concentration of surfactant compared to the high oil content (as all the products had a same oil content).

Drug release study

Analyses were conducted to evaluate the drug release from different optimized formulations and pure LG. Drug release from SLN was exceedingly significant ($p < 0.01$) in comparison with pure LG (Table 4). A rapid release of drug from LG_{SLN1} was observed, as 71.65% of the drug was liberated in 24 h. Other products exhibited comparatively slow-release pattern [LG_{SLN2} (68.36) > LG_{SLN3} (63.97), > LG_{SLN4} (52.69) > LG_{SLN5} (48.86)] compared to LG_{SLN1} in 24 h, while neat LG was very low (30% in 24 h). This finding reflects the fact that SLN formulations with smaller particle sizes have more surface area, allowing for faster dissolution and higher releases.

In vitro skin permeation studies

The penetration potential of the drug (LG) from the optimal formulations and pure LG were compared by skin permeation study. In vitro skin permeation exhibited highest for LG_{SLN1} and lowest by the pure LG (control) (Fig. 3). Highest release was exhibited by LG_{SLN1}. It might be due to its smallest droplet size and lesser viscosity as equated to other developed products (LG_{SLN1} > LG_{SLN2} > LG_{SLN4} > LG_{SLN3} > LG_{SLN5} > pure LG). In the lipid route of the stratum corneum (SC), the neutral lipids are organized as bilayers with their lipophilic chains fronting each other to produce a lipophilic bimolecular layer, is thought to be the mechanism by which SLNs improve drug permeation through the skin (Lertsatitthanakorn et al. 2006). Drug available in the lipidic domain of SLN penetrates directly into the SC, upsetting its bilayer configuration in conjunction with the surfactant on the surface, in increased lipid route permeability to the drug. Alternatively, its hydrophilic site hydrates the SC deeply, which is particularly significant in the process of percutaneous drug absorption (Thomas et al 2017; Faiyazuddin et al 2010b). Majority of the lipophilic drugs follow the lipid pathway for percutaneous permeation (Lertsatitthanakorn et al. 2006; Zouboulis 2001). LG being lipophilic in nature, has the tendency to pass through the preexisting lipidic pathway more efficiently (Sinha et al. 2019). SLN is an outstanding vehicle for its increased percutaneous LG uptake because of its smaller size and lower viscosity spectrum (Fang et al. 2008). Citral, which is a crucial constituent of LG and is a well-known permeability enhancer (Irfan et al. 2022; Rauber et al. 2005), can enable SLNs to more permeable following topical application.

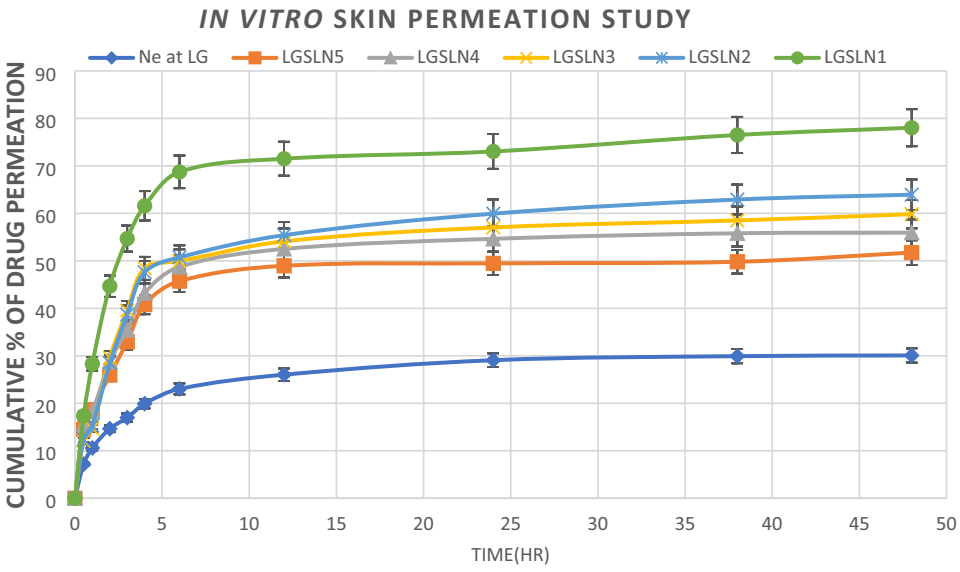

Fig. 3 In vitro skin permeation profile of LG in SLN dispersions, ($n = 3$)

Permeability data (Table 6) revealed that there was a remarkable enhancement in the steady-state flux (J_{ss}), permeability coefficient (K_p) and enhancement ratio (E_r) of optimized SLNs as compared to pure LG ($p < 0.05$). Better permeation of LG oil from LG_{SLN1} could be mainly attributed to the combined effects of permeation enhancers including citral, Tween 80 and ethanol, as well as the least droplet size and lowest viscosity. Permeability parameters of all the SLNs and neat LG are given in Table 6.

Stability study at different storage temperature

Literature suggests that temperature has effects on particle size and zeta potential, which was studied here also. All the formulations were placed in glass vials and stored at diverse stressed conditions (4 °C, 25 °C and 50 °C) for three months. A miniature increase in droplet size was observed at 4 °C and 25 °C but a significant increase in size was obtained at 50 °C. The mean particle diameter of the LG_{SLN1} stored at 50 °C was increased from 142.8 to 183.19 nm in three months, whereas 146.6 nm and 148.5 nm were observed when stored at 4 °C and 25 °C, respectively (Table 5). The result sturdily corroborates the shielding aptitude of Tween-80 at moderate temperatures. Similar results were also predicted in the case of other formulations (size: 50 °C > 25 °C > 4 °C). These judgments are also corroborated by ZP data obtained for the formulations maintained at different temperature conditions (Table 5). Based on the foregoing data, the process of particle accumulation was intensified by increasing the storage temperatures. This is related to the destabilization of SLN dispersions as a result of increasing input energy from higher temperatures. The provided energy boosts the particles' kinetic energy and encourages collisions, resulting in particle aggregation. Other factor could be the temperature-dependent performance of the surfactant coating on the particle surface. Because of the preferential production of platelet-shaped particles as a characteristic of the modification, the particle surface area increased when the polymorphic alterations of the lipid particles changed over time. Particle growth stemmed from the surfactant molecules' inability to provide an adequate coating to the newer particle surfaces formed. FTIR research was conducted to check for any potential incompatibilities between the LG oil and other formulation ingredients (Tween 80 and stearic acid). The results revealed that LG oil and other additives did not interact in any way and were compatible with one another (S2).

Table 6 Permeability parameters of different LG-SLN formulations and neat LG ($n = 3$)

Formulation matrices	$J_{ss} \pm$ SD (mg/cm^2/h)	$K_p \pm$ SD (cm/h) $\times 10^2$	E_r
Pure LG	0.0454 ± 0.021	0.0507 ± 0.0091	–
LG_{SLN1}	0.6133 ± 0.0361	0.4573 ± 0.0141	13.50
LG_{SLN2}	0.5535 ± 0.0285	0.3096 ± 0.0134	12.19
LG_{SLN3}	0.3303 ± 0.0290	0.3691 ± 0.0162	7.27
LG_{SLN4}	0.2504 ± 0.0310	0.1712 ± 0.0103	5.51
LG_{SLN5}	0.2753 ± 0.1610	0.3063 ± 0.0216	6.064

J_{ss} steady-state flux, K_p permeability coefficient, E_r enhancement ratio

Conclusions

Based on the lowest droplet size, minimum polydispersity, lowest viscosity, appreciable drug release behavior and increased skin permeation profile, LG_{SLN1} was taken as optimized solid lipid nanoparticle formulation containing lipid phase 10% w/w, Tween 80, ethanol and distilled water for topical applications. From in vitro outcomes, it can be concluded that the established SLN could be an auspicious vehicle for enhanced topical delivery of LG oil. The observed results also indicate the fact that the phyto-cosmeceutical perspective of the nanolipidic carrier for topical administration of LG oil utilizing pharmaceutically acceptable components can be further explored in the future for widespread clinical applicability.

Supplementary Information The online version contains supplementary material available at https://doi.org/10.1007/s13205-023-03726-5.

Acknowledgements Authors are thankful to the Taif University Researchers Supporting Project (Number TURSP-2020/124), Taif University, Taif, Saudi Arabia, for supporting this work.

Author contributions The authors confirm their contribution as follows: study conception and design: AbA, and AmA; data collection and analysis: MHW, WA, MA, and SAHA; interpretation of results: WA, AbA and AmA; draft manuscript preparation: MA, AbA, and SAHA; Funding acquisition: AbA.

Funding This research was funded by Taif University Research Supporting Project number 'TURSP-2020/124.'

Data availability The authors confirm that the data supporting the study's findings are included in the article.

Declarations

Conflict of interest The authors declare no conflict of interest.

Ethical approval The study was approved by Ethics Committee, Taif University, Saudi Arabia.

References

Al-Harrasi A, Bhatia S, Behl T, Kaushik D (2022) Effects of essential oils on CNS. Role of essential oils in the management of COVID-19. CRC Press, Boca Raton, pp 269–297

Ali A, Ali A, Rahman MA, Warsi MH, Yusuf M, Alam P (2022) Development of nanogel loaded with lidocaine for wound-healing: illustration of improved drug deposition and skin safety analysis. Gels 8(8):466

Ascenso A, Ribeiro HM, Marques HC, Simoes S (2011) Topical delivery of antioxidants. Curr Drug Deliv 8:640–660

Bhaskar K, Anbu J, Ravichandiran V, Venkateswarlu V, Rao YM (2009) Lipid nanoparticles for transdermal delivery of flurbiprofen: formulation, in vitro, ex vivo and in vivo studies. Lipids Health Dis 8:6

Chen H, Zhong Q (2022) Physical and antimicrobial properties of self-emulsified nanoemulsions containing three synergistic essential oils. Int J Food Microbiol 365:109557

Cui HY, Wu J, Lin L (2016) Inhibitory effect of liposome-entrapped lemongrass oil on the growth of Listeria monocytogenes in cheese. Int J Dairy Sci 99(8):6097–6104

Dingler A, Gohla S (2002) Production of solid lipid nanoparticles (SLN): scaling up feasibilities. J Microencapsul 19:11–16

Dolatabadi JEN, Valizadeh H, Hamishehkar H (2015) Solid lipid nanoparticles as efficient drug and gene delivery systems: recent breakthroughs. Adv Pharm Bull 5:151–159

Faheem F, Liu ZW, Rabail R, Haq IU, Gul M, Bryła M, Roszko M, Kieliszek M, Din A, Aadil RM (2022) Uncovering the industrial potentials of Lemongrass essential oil as a food preservative: a review. Antioxidants 11:720

Faiyazuddin M, Ahmad N, Baboota S, Ali J, Ahmad S, Akhtar J (2010a) Chromatographic analysis of trans and cis-citral in lemongrass oil and in a topical phytonanocosmeceutical formulation, and validation of the method. J Planar Chromatogr 23:233–236

Faiyazuddin M, Akhtar N, Akhter J, Suri S, Shakeel F, Shafiq S, Mustafa G (2010b) Production, characterization, in vitro and ex vivo studies of babchi oil-encapsulated nanostructured solid lipid carriers produced by a hot aqueous titration method. Pharmazie 65:348–355

Fang JY, Fang CL, Liu CH, Su YH (2008) Lipid nanoparticles as vehicles for topical psoralen delivery: solid lipid nanoparticles (SLN) versus nanostructured lipid carriers (NLC). Eur J Pharm Biopharm 70(2):633–640

Freitas C, Müller RH (1999) Correlation between long-term stability of solid lipid nanoparticles (SLN™) and crystallinity of the lipid phase. Eur J Pharm Biopharm 47:125–132

Holland DB, Jeremy AH (2005) The role of inflammation in the pathogenesis of acne and acne scarring. Semin Cutan Med Surg 24:79–83

Irfan S, Zahra SM, Murtaza MA, Zainab S, Shafique B, Kanwal R, Roobab U, Ranjha MM (2022) Characterization of lemongrass oleoresins. Handbook of oleoresins. CRC Press, New York, pp 261–283

Jaber AA, Mirza MA, Anwer MK, Alshetaili AS, Alshahrani SM, Al-Shdefat RI, Talegaonkar S, Iqbal Z (2018) Mucoadhesive gels loaded with Ciclopirox olamine containing SLN for sustained vaginal drug delivery: in vitro and in vivo characterization. Lat Am J Pharm 37(2):388–400

Jenning V, Thünemann AF, Gohla SH (2000) Characterisation of a novel solid lipid nanoparticle carrier system based on binary mixtures of liquid and solid lipids. Int J Pharm 199:167–177

Jenning V, Lippacher A, Gohla SH (2002) Medium scale production of solid lipid nanoparticles (SLN) by high pressure homogenization. J Microencapsul 19:1–10

Kumar PS, Nattudurai G, Islam VI, Ignacimuthu S (2022) The effects of some essential oils on Alternaria alternata, a post-harvest phyto-pathogenic fungus in wheat by disrupting ergosterol biosynthesis. Phytoparasitica 50:513–525

Lertsatitthanakorn P, Taweechaisupapong S, Aromdee C, Khunkitti W (2006) In vitro bioactivities of essential oils used for acne control. Int J Aromather 16:43–49

Li P, Amit K, Wagner GA, RF, Krill S, Joshi YM, Serajuddin AT, (2005) Effect of combined use of non-ionic surfactants on formation of oil-in-water microemulsions. Int J Pharm 288:27–34

Liedtke S, Wissing S, Müller RH, Mäder K (2000) Influence of high pressure homogenisation equipment on nanodispersions characteristics. Int J Pharm 196:183–185

Ma JY, Hasham R, Abd Rasid ZI, Noor NM (2021) Formulation and characterization of nanostructured lipid carrier encapsulate lemongrass oil using ultrasonication technique. Chem Eng Trans 83:475–480

Masurkar SA, Chaudhari PR, Shidore VB, Kamble SP (2011) Rapid biosynthesis of silver nanoparticles using *Cymbopogan citratus* (lemongrass) and its antimicrobial activity. Nano-Micro Lett 3(3):189–194

Mirza MA, Ahmad S, Mallick MN, Manzoor N, Talegaonkar S, Iqbal Z (2013) Development of a novel synergistic thermosensitive gel for vaginal candidiasis: an in vitro, in vivo evaluation. Colloids Surf B Biointerfaces 103:275–282

Mukarram M, Choudhary S, Khan MA, Poltronieri P, Khan MMA, Ali J, Kurjak D, Shahid M (2021) Lemongrass essential oil components with antimicrobial and anticancer activities. Antioxidants (basel) 11(1):20

Muller RH, Lucks JS (1996) European Patent EP 0605497

Onawunmi GO, Yisak WA, Ogunlana EOJ (1984) Antibacterial constituents in the essential oil of *Cymbopogon citratus* (DC.) Stapf. Ethnopharmacol 12:279–283

Qadir A, Faiyazuddin MD, Hussain MT, Alshammari TM, Shakeel F (2016) Critical steps and energetics involved in a successful development of a stable nanoemulsion. J Mol Liq 214:7–18

Rauber CS, Guterres SS, Schapoval EES (2005) LC determination of citral in *Cymbopogon citratus* volatile oil. J Pharma Biomed Anal 37:597–601

Salvia-Trujillo L, Rojas-Graü MA, Soliva-Fortuny R, Martín-Belloso O (2014) Impact of microfluidization or ultrasound processing on the antimicrobial activity against *Escherichia coli* of lemongrass oil-loaded nanoemulsions. Food Control 37:292–297

Sinha P, Srivastava N, Rai VK, Mishra R, Ajayakumar PV, Yadav NP (2019) A novel approach for dermal controlled release of salicylic acid for improved anti-inflammatory action: combination of hydrophilic-lipophilic balance and response surface methodology. J Drug Deliv Sci Technol 52:870–884

Souza VVMA, Almeida JM, Barbosa LN, Silva NCC (2022) Citral, carvacrol, eugenol and thymol: antimicrobial activity and its application in food. J Essent Oil Res 34(3):181–194

Thatipamula RP, Palem CR, Gannu R, Mudragada S, Yamsani MR (2011) Formulation and in vitro characterization of domperidone loaded solid lipid nanoparticles and nanostructured lipid carriers. Daru J Faculty Pharm Tehran Univ Med Sci 19(1):23

Thomas L, Zakir F, Mirza MA, Anwer MK, Ahmad FJ, Iqbal Z (2017) Development of Curcumin loaded chitosan polymer based nanoemulsion gel: In vitro, ex vivo evaluation and in vivo wound healing studies. Int J Biol Macromol 101:569–579

Trotta M, Debernardi F, Caputo O (2003) Preparation of solid lipid nanoparticles by a solvent emulsification-diffusion technique. Int J Pharm 257:153–160

Valková V, Ďúranová H, Galovičová L, Borotová P, Vukovic NL, Vukic M, Kačániová M (2022) *Cymbopogon citratus* Essential Oil: its application as an antimicrobial agent in food preservation. Agronomy 12:155

Yadav V, Mahor A, Prajapati S, Alok S, Verma A, Kumar N, Kumar S (2014) Solid lipid nanoparticles (sln): formulation by high pressure homogenization. World J Pharmacy Pharm Sci 3:1200–1203

Yuan H, Huang LF, Du YZ, Ying XY, You J, Hu FQ, Zeng S (2008) Solid lipid nanoparticles prepared by solvent diffusion method in a nanoreactor system. Colloids Surf B Biointerfaces 61:132–137

Zakir F, Ahmad A, Mirza MA, Kohli K, Ahmad FJ (2021) Exploration of a transdermal nanoemulgel as an alternative therapy for post-menopausal osteoporosis. J Drug Deliv Sci Technol 65:102745

Zhao M, Zhang Y, Zou C, Dai C, Gao M, Li Y, Lv W, Jiang J, Wu Y (2017) Can more nanoparticles induce larger viscosities of nanoparticle-enhanced wormlike micellar system (NEWMS)? Materials 10(9):1096

Zouboulis C (2001) Exploration of retinoid activity and the role of inflammation in acne: issues affecting future directions for acne therapy. J Eur Acad Dermatol Venereol 15:63–67